

Steady-State Modeling of SVC and TCSC for Power Flow Analysis

Mohammed Osman Hassan, S. J. Cheng, Senior Member, IEEE, Zakaria Anwar Zakaria

Abstract— in this paper steady-state modeling of Static VAR Compensator (SVC) and Thyristor Controlled Series Compensator (TCSC) for power flow studies has been represented and discussed in details. Firing angle model for SVC was proposed to control the voltage at which it is connected. In same manner firing angle model for TCSC is used to control active power flow of the line to which TCSC is installed. The proposed models take firing angle as state variable in power flow formulation. To validate the effectiveness of the proposed models Newton-Raphson method algorithm was developed to solve power flow equations in presence of SVC and TCSC. Case studies are carried out on 9-bus test system to demonstrate the performance of the proposed models.

Index Terms— Newton-Raphson, Power Flow, Static VAR Compensator, Steady-state modeling, Thyristor Controlled Series Compensator.

I. INTRODUCTION

With the rapid development of power system, especially the increased use of transmission facilities due to higher industrial output and deregulation, it becomes necessary to explore new ways of maximizing power transfer in existing transmission facilities, while at the same time maintaining the acceptable levels of the network reliability and stability. On the other hand, the fast development of power electronic technology has made FACTS (flexible AC Transmission system) promising solution of future power system. FACTS controllers such as Static Synchronous Compensator (STATCOM), Static VAR Compensator (SVC), Thyristor Controlled Series Compensator (TCSC), Static Synchronous Series Compensator (SSSC) and Unified Power Flow controller (UPFC) are able to change the network parameters in a fast and effective way in order to achieve better system performance [1], [2], [3], [4]. These controllers are used for enhancing dynamic performance of power systems in terms of voltage/angle stability while improving the power transfer capability and voltage profile in steady-state conditions [5], [6], [7], [8], [9].

Manuscript received December 31, 2008. This work was supported by Huazhong University of science and technology.

Mohammed Osman Hassan, Ph.D student -Department of electrical engineering - Huazhong University of Science and Technology - Wuhan-china - Tel: 0082762205767 -Email: osman_zain12@yahoo.com

S. J. Cheng, Senior Member, IEEE - Department of electrical engineering - Huazhong University of Science and Technology - Wuhan-china - Email: sjcheng@mail.hust.edu.cn.

Zakaria Anwar Zakaria -Ph.D student - School of Electrical Engineering- Wuhan University - Wuhan-china - Email: zakariaaz@yahoo.com.

Static VAR Compensator (SVC) and Thyristor Controlled Series Compensator (TCSC) are FACTS controllers based on thyristor controlled reactor (TCRs), the first is a shunt compensator used for voltage regulation which is achieved by controlling the production, absorption and flow of reactive power through the network. The later is a series compensator, which allows rapid and continuous changes of transmission impedance, controlling power flow in the line and improving system stability.

Now, for maximum utilization of any FACTS device in power system planning, operation and control, power flow solution of the network that contains any of these devices is a fundamental requirement. As a result, many excellent research works have been carried out in the literature for developing efficient load flow algorithm for FACTS devices [10], [11], [12], [13], [14].

This paper focuses on the development of SVC and TCSC models and their implementation in Newton-Raphson load flow algorithm, to control voltage of the bus and active power across the line. Incorporation of FACTS devices in an existing power flow algorithm results in increased complexity of programming due to the following reasons:

- New terms owing to the contributions from the FACTS devices need to be included in the existing power flow equations of the concerned buses. These terms necessitate modification of existing power flow codes.
- New power flow equations related to the FACTS devices come into the picture, which dictate formulation of separate subroutine(s) for computing them.
- The system Jacobian matrix contains entirely new Jacobian sub-blocks exclusively related to the FACTS devices. Therefore, new codes have to be written for computation of these Jacobian sub-blocks.

In section (II) of this paper derivation of power flow equation for two-port network under steady state conditions is represented, while section (III) demonstrates the modeling of SVC. The rest of the sections are organized as follows: in section (IV) modeling of TCSC is presented. The simulation and results are presented in section (V). Finally; conclusion is discussed in section (VI).

II. POWER FLOW EQUATION

Basically power flow problem involves solving the set of non-linear algebraic equations which represent the network under steady state conditions. Newton-type methods, with their strong convergence characteristics, have proved most successful to solve power flow problem. To illustrate the power flow equations, the power flow across the general two-port network element connecting buses k and m shown in Fig. 1 is considered and the following equations are obtained.

The injected active and reactive powers at bus-k (P_k and Q_k) are:

$$P_k = G_{kk}V_k^2 + (G_{km} \cos \delta_{km} + B_{km} \sin \delta_{km})V_kV_m \dots\dots\dots (1)$$

$$Q_k = -B_{kk}V_k^2 + (G_{km} \sin \delta_{km} - B_{km} \cos \delta_{km})V_kV_m \dots\dots\dots (2)$$

$$P_m = G_{mm}V_m^2 + (G_{mk} \cos \delta_{mk} + B_{mk} \sin \delta_{mk})V_kV_m \dots\dots\dots (3)$$

$$Q_m = -B_{mm}V_m^2 + (G_{mk} \sin \delta_{mk} - B_{mk} \cos \delta_{mk})V_kV_m \dots\dots\dots (4)$$

Where $\delta_{km} = \delta_k - \delta_m = -\delta_m$; $Y_{kk} = Y_{mm} = G_{kk} + jB_{kk} = Y_{ko} + Y_{km}$ and $Y_{km} = Y_{mk} = G_{km} + jB_{km} = -Y_{mk}$

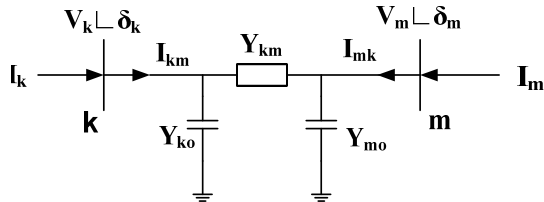


Fig.1 General two-port network

The nodal power flow equations, $P=f(V,\theta,G,B)$ and $Q=g(V,\theta,G,B)$ (4) and their linearisation around a base point, (P^0, Q^0)

$$\begin{bmatrix} \Delta P \\ \Delta Q \end{bmatrix}^i = \begin{bmatrix} J \end{bmatrix}^i \begin{bmatrix} \Delta \theta \\ \Delta V \end{bmatrix}^i \dots\dots\dots (5)$$

The variables used in equations (4, 5) are:
 P and Q are vectors of real and reactive nodal power injections as a function of nodal voltage magnitudes V and angles θ , and network conductances G and susceptances B .
 $\Delta P = P_{spec} - P_{cal}$ is the real power mismatch vector.
 $\Delta Q = Q_{spec} - Q_{cal}$ is the reactive power mismatch vector.
 $\Delta \theta$ and ΔV are the vectors of incremental changes in nodal voltage magnitudes and angles.
 J is the matrix of partial derivatives of real and reactive powers with respect to voltage magnitudes and angles.
 i indicates the iteration number.

III. MODELING OF STATIC VAR COMPENSATOR

Static VAR Compensator (SVC) is a shunt connected FACTS controller whose main functionality is to regulate the voltage at a given bus by controlling its equivalent reactance. Basically it consists of a fixed capacitor (FC) and a thyristor controlled reactor (TCR). Generally they are two configurations of the SVC.

A) SVC total susceptance model. A changing susceptance B_{svc} represents the fundamental frequency equivalent susceptance of all shunt modules making up the SVC as shown in Fig. 2 (a).

B) SVC firing angle model. The equivalent reactance X_{SVC} , which is function of a changing firing angle α , is made up of the parallel combination of a thyristor controlled reactor (TCR) equivalent admittance and a fixed capacitive reactance as shown in Fig. 2 (b). This model provides information on the SVC firing angle required to achieve a given level of compensation.

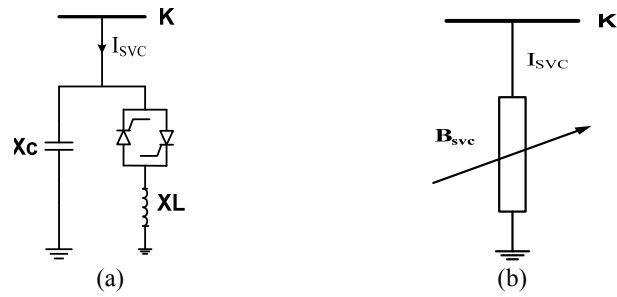


Fig.2 (a) SVC firing angle model (b) SVC total susceptance model

Figure.3 shows the steady-state and dynamic voltage-current characteristics of the SVC. In the active control range, current/susceptance and reactive power is varied to regulate voltage according to a slope (droop) characteristic. The slope value depends on the desired voltage regulation, the desired sharing of reactive power production between various sources, and other needs of the system. The slope is typically 1-5%. At the capacitive limit, the SVC becomes a shunt capacitor. At the inductive limit, the SVC becomes a shunt reactor (the current or reactive power may also be limited). [14].

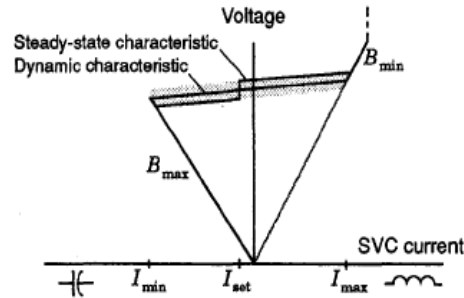


Fig.3 steady-state and dynamic voltage/current characteristics of the SVC

SVC firing angle model is implemented in this paper. Thus, the model can be developed with respect to a sinusoidal voltage, differential and algebraic equations can be written as $I_{SVC} = -jB_{SVC}V_k$ (6)

The fundamental frequency TCR equivalent reactance X_{TCR}

$$X_{TCR} = \frac{\pi X_L}{\sigma - \sin \sigma} \dots\dots\dots (7)$$

Where $\sigma = 2(\pi - \alpha)$, $X_L = \omega L$
 And in terms of firing angle

$$X_{TCR} = \frac{\pi X_L}{2(\pi - \alpha) + \sin(2\alpha)} \dots\dots\dots (8)$$

σ and α are conduction and firing angles respectively.
 At $\alpha=90^\circ$, TCR conducts fully and the equivalent reactance X_{TCR} becomes X_L , while at $\alpha=180^\circ$ TCR is blocked and its equivalent reactance becomes infinite.

The SVC effective reactance X_{SVC} is determined by the parallel combination of X_C and X_{TCR}

$$X_{SVC} = \frac{\pi X_C X_L}{X_C [2(\pi - \alpha) + \sin 2\alpha] - \pi X_L} \dots\dots\dots (9)$$

Where $X_C = 1/\omega C$

$$Q_k = -V_k^2 \left\{ \frac{X_C [2(\pi - \alpha) + \sin 2\alpha] - \pi X_L}{\pi X_C X_L} \right\} \dots\dots (10)$$

The SVC equivalent reactance is given by (9). It is shown in Fig. 4 that the SVC equivalent susceptance ($B_{SVC} = -1/X_{SVC}$) profile, as function of firing angle, does not present discontinuities, i.e., B_{SVC} varies in a continuous, smooth fashion in both operative regions. Hence, linearization of the SVC power flow equations, based on B_{SVC} with respect to firing angle, will exhibit a better numerical behavior than the linearized model based on X_{SVC} .

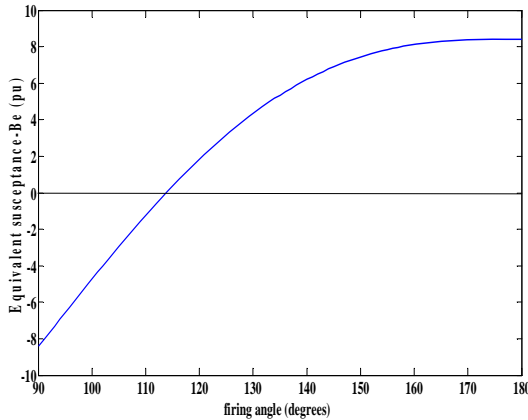


Fig.4 SVC equivalent susceptance profile

The initialization of the SVC variables based on the initial values of ac variables and the characteristic of the equivalent susceptance (Fig.4), thus the impedance is initialized at the resonance point $X_{TCR} = X_C$, i.e. $Q_{SVC} = 0$, corresponding to firing angle 115° , for chosen parameters of L and C i.e. $X_L = 0.1134 \Omega$ and $X_C = 0.2267 \Omega$.

Proposed SVC power flow model:

The proposed model takes firing angle as the state variable in power flow formulation. From equation (10) the SVC linearized power flow equation can be written as

$$\begin{bmatrix} \Delta P_k \\ \Delta Q_k \end{bmatrix}^{(i)} = \begin{bmatrix} 0 & 0 \\ 0 & \frac{2V_k^2}{\pi X_L} [\cos(2\alpha) - 1] \end{bmatrix}^{(i)} \begin{bmatrix} \Delta \theta_k \\ \Delta \alpha \end{bmatrix}^{(i)} \dots (11)$$

At the end of iteration i, the variable firing angle α is updated according to

$$\alpha^{(i)} = \alpha^{(i-1)} + \Delta \alpha^{(i)} \dots\dots\dots (12)$$

IV. MODELING OF THYRISTOR CONTROLLED COMPENSATER

Thyristor-controlled series capacitor (TCSC) allows rapid and continuous changes of transmission line impedance. Fig.5 shows the TCSC module connected in series with the transmission line. The structure of the controller is equivalent to the FC-TCR SVC. However, the equivalent impedance of the TCSC at 60 Hz is more appropriately represented by assuming a sinusoidal steady-state total current rather than a sinusoidal voltage.

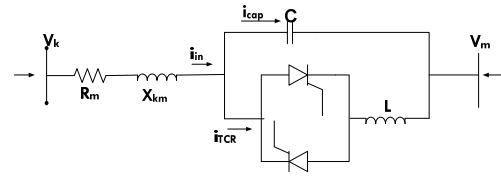


Fig.5 TCSC module

In this paper TCSC is represented by its fundamental frequency impedance. The TCSC linearized power flow equations, with respect to the firing angle, are incorporated into an existing Newton-Raphson algorithm. Since the explicit information about the TCSC impedance-firing angle is available, good initial conditions are easily selected, hence preventing power flow iterative process from entering the nonoperative regions owing to the presence of resonant bands. The fundamental TCSC equivalent reactance is given as

$$X_{TCSC} = -X_C + K_1(2\sigma + \sin 2\sigma - K_2 \cos^2 \sigma (\varpi \tan \varpi \sigma) - \tan \sigma) \dots\dots\dots (13)$$

Where

$$\sigma = \pi - \alpha, \quad \varpi = \sqrt{\frac{X_C}{X_L}}$$

$$X_{LC} = \frac{X_C X_L}{X_C - X_L}, K_1 = \frac{X_C + X_{LC}}{\pi}, K_2 = \frac{(X_{LC})^2}{\pi X_L} \dots (14)$$

Fig. 6 shows the TCSC equivalent reactance as a function of firing angle in the range of 90-180°.

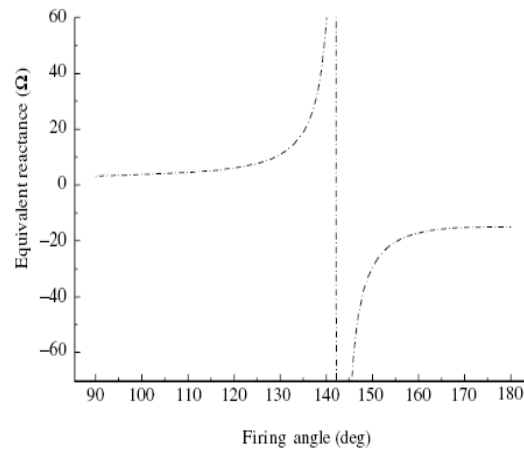


Fig.6. TCSC equivalent Reactance as a function of firing angle

The behavior of TCSC power flow model is influenced greatly by the number of resonant points which can be given as

$$\alpha = \pi \left(1 - \frac{(2n-1)\omega\sqrt{LC}}{2} \right) \dots\dots\dots (15)$$

Where n=1, 2, 3....

As shown in Fig. 6 resonant point exists at $\alpha_{res} = 142.8$, for chosen parameters of L and C i.e. $X_L = 2.6 \Omega$ and $X_C = 15 \Omega$. It should be noted that near resonant point, a small variations in the firing angle will induce large changes in both X_{TCSC} and

$\partial X_{tcsc}/\partial \alpha$. This in turn may lead to ill conditioned TCSC power equations

Proposed TCSC power flow model:

Transmission line admittance in which TCSC is connected can be written as

$$G_{tcsc} + jB_{tcsc} = \frac{1}{R + j(X + X_{tcsc})} \dots\dots\dots (16)$$

This line admittance is incorporated in bus admittance matrix, and remaining steps are carried out as follows. Power flow equations of the line k-m in which TCSC is placed is given by

$$P_{km}^{atcsc} = V_k^2 G_{tcsc} - V_k V_m \left(G_{tcsc} \cos(\delta_{km}) + B_{tcsc} \sin(\delta_{km}) \right) \dots\dots\dots (17)$$

When TCSC is used to control power flow in the line k-m, the set of linearised power flow equations are given by

$$\begin{bmatrix} \Delta P_k \\ \Delta P_m \\ \Delta Q_k \\ \Delta Q_m \\ \Delta P_{km}^{atcsc} \end{bmatrix} = \begin{bmatrix} \frac{\partial P_k}{\partial \theta_k} & \frac{\partial P_k}{\partial \theta_m} & \frac{\partial P_k}{\partial V_k} V_k & \frac{\partial P_k}{\partial V_m} V_m & \frac{\partial P_k}{\partial \alpha} \\ \frac{\partial P_m}{\partial \theta_k} & \frac{\partial P_m}{\partial \theta_m} & \frac{\partial P_m}{\partial V_k} V_k & \frac{\partial P_m}{\partial V_m} V_m & \frac{\partial P_m}{\partial \alpha} \\ \frac{\partial Q_k}{\partial \theta_k} & \frac{\partial Q_k}{\partial \theta_m} & \frac{\partial Q_k}{\partial V_k} V_k & \frac{\partial Q_k}{\partial V_m} V_m & \frac{\partial Q_k}{\partial \alpha} \\ \frac{\partial Q_m}{\partial \theta_k} & \frac{\partial Q_m}{\partial \theta_m} & \frac{\partial Q_m}{\partial V_k} V_k & \frac{\partial Q_m}{\partial V_m} V_m & \frac{\partial Q_m}{\partial \alpha} \\ \frac{\partial P_{km}^{atcsc}}{\partial \theta_k} & \frac{\partial P_{km}^{atcsc}}{\partial \theta_m} & \frac{\partial P_{km}^{atcsc}}{\partial V_k} V_k & \frac{\partial P_{km}^{atcsc}}{\partial V_m} V_m & \frac{\partial P_{km}^{atcsc}}{\partial \alpha} \end{bmatrix} \begin{bmatrix} \Delta \theta_k \\ \Delta \theta_m \\ \frac{\Delta V_k}{V_k} \\ \frac{\Delta V_m}{V_m} \\ \Delta \alpha \end{bmatrix} \dots\dots\dots (18)$$

Where, the elements of additional row and column of the modified Jacobean can be written as:

$$\frac{\partial P_k}{\partial \alpha} = V_k V_m \left(-\frac{\partial G_{tcsc}}{\partial \alpha} \cos(\delta_{km}) - \frac{\partial B_{tcsc}}{\partial \alpha} \sin(\delta_{km}) \right) - V_k^2 \frac{\partial X_{tcsc}}{\partial \alpha} \dots\dots\dots (19)$$

$$\frac{\partial Q_k}{\partial \alpha} = V_k V_m \left(-\frac{\partial G_{tcsc}}{\partial \alpha} \sin(\delta_{km}) - \frac{\partial B_{tcsc}}{\partial \alpha} \cos(\delta_{km}) \right) - V_k^2 \frac{\partial X_{tcsc}}{\partial \alpha} \dots\dots\dots (20)$$

where

$$\frac{\partial G_{tcsc}}{\partial \alpha} = \frac{-2R(X + X_{tcsc})}{(R^2 + (X + X_{tcsc})^2)^2} \frac{\partial X_{tcsc}}{\partial \alpha} \dots\dots\dots (21)$$

$$\frac{\partial B_{tcsc}}{\partial \alpha} = -\frac{1}{R^2 + (X + X_{tcsc})^2} \left(\frac{\partial X_{tcsc}}{\partial \alpha} \right) + \frac{2(X + X_{tcsc})^2}{(R^2 + (X + X_{tcsc})^2)^2} \left(\frac{\partial X_{tcsc}}{\partial \alpha} \right) \dots\dots\dots (22)$$

$$\frac{\partial X_{tcsc}}{\partial \alpha} = -2C_1(1 + \cos 2\alpha) + C_2 \sin(2\alpha) \left(\varpi \tan(\varpi(\pi - \alpha)) + \tan \alpha \right) + C_2 \left(\varpi^2 \frac{\cos^2(\pi - \alpha)}{\cos^2(\varpi(\pi - \alpha))} - 1 \right) \dots\dots\dots (23)$$

Also the elements of the added row in the modified Jacobean matrix (18)

$$\frac{P_{km}^{atcsc}}{\partial \alpha} = V_k^2 \frac{G_{tcsc}}{\partial \alpha} - V_k V_m \left(\frac{G_{tcsc}}{\partial \alpha} \cos(\delta_{km}) + \frac{B_{tcsc}}{\partial \alpha} \sin(\delta_{km}) \right) \dots\dots\dots (24)$$

$$\frac{P_{km}^{atcsc}}{\partial \delta_k} = -V_k V_m \left(-G_{tcsc} \sin(\delta_{km}) + B_{tcsc} \cos(\delta_{km}) \right) \dots\dots\dots (25)$$

$$\frac{\partial P_{km}^{atcsc}}{\partial \delta_m} = \frac{\partial P_{km}^{atcsc}}{\partial \delta_k} \dots\dots\dots (26)$$

$$\frac{\partial P_{km}^{atcsc}}{\partial V_k} V_k = P_{km}^\alpha + V_k^2 G_{tcsc} \dots\dots\dots (27)$$

$$\frac{\partial P_{km}^{atcsc}}{\partial V_m} V_m = P_{km}^{atcsc} - V_k^2 G_{tcsc} \dots\dots\dots (28)$$

In the mismatch vector of (18)

$\Delta P_{km}^{atcsc} = P_{km}^{reg} - P_{km}^{atcsc}$ is the active power flow mismatch for the TCSC module. P_{km}^{reg} is the required power flow in the TCSC branch.

Now solve for system variables along with the firing angle mismatch using (18), making use of modified Jacobean matrix. Update the firing angles using the following equation $\alpha^{i+1} = \alpha^i + \Delta \alpha$, Where $\Delta \alpha$ is the incremental change in the TCSC's firing angle and i shows ith iteration.

V. SIMULATION AND RESULTS

9-bus test system is used to assess the effectiveness of SVC and TCSC models developed in this paper. Fig.7 below show the single line diagram of system, with 230 kv and 100MVA base has been considered. The data of system can be found in [15]. Four cases are considered, SVC is connected at bus 8 and, then at bus6, TCSC connected between line 7-8 and, then between line 9-8.

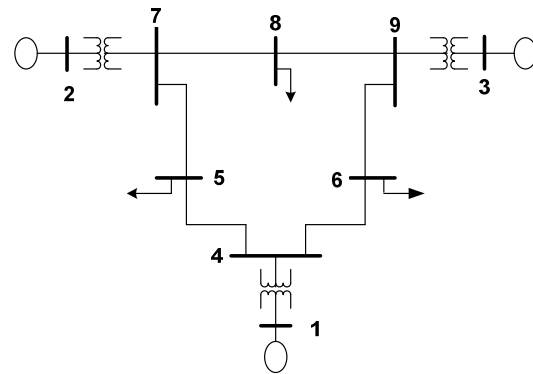


Fig.7 9-bus test system

Case I:

SVC is connected to bus 8, the control aim to keep the voltage at that bus at 1.0 pu. The of values X_C and X_L are chosen as 1.4 pu and 0.28 pu, firing angle is set initially at 145° , which lies on the capacitive region of SVC . The convergent is obtained after 6 iterations. SVC absorbs 21.86 MAVR from bus 8 in order to keep the voltage magnitude at 1 pu, with final firing angle of 128.56° and B_{SVC} equal to -0.2186 pu. Table (1) gives the voltage magnitude and phase angle for all buses of the system with and without SVC.

Case II:

SVC is connected to bus 6, to keep the voltage at bus 6 at 1.0 pu. The of values X_C and X_L are chosen as 0.293 pu and 0.059 pu, firing angle is set initially at 125° , which lies on the

capacitive region of SVC . The convergent is obtained after 6 iterations. SVC absorbs 13.72 MAVR from bus 6 in order to keep the voltage magnitude at 1 pu, with final firing angle of 132.72° and B_{SVC} equal to -0.1372 pu. The voltage magnitude and phase angle for all buses of the system with SVC are given in table (1).

Table (1) Voltage magnitude and phase angle for 9-bus test system with and without SVC

Bus	Without FACTS		SVC at bus 8		SVC at bus 6	
1	1.0400	0	1.0400	0	1.0400	0
2	1.0250	9.2800	1.0250	9.4248	1.0250	9.2759
3	1.0250	4.6648	1.0250	4.7394	1.0250	4.6707
4	1.0258	-2.217	1.0236	-2.2257	1.0213	-2.2290
5	0.9956	-3.989	0.9916	-3.9983	0.9920	-4.0201
6	1.0127	-3.687	1.0092	-3.6956	1.0000	-3.6458
7	1.0258	3.7197	1.0189	3.8269	1.0243	3.7077
8	1.0159	0.7275	1.0000	0.8268	1.0138	0.7114
9	1.0324	1.9667	1.0269	2.0270	1.0295	1.9650

Case III:

TCSC is connected between bus7 and bus8. The objective control is increase the active power of that line to 80 MW. The value of x_L was chosen as 9.52Ω i.e.(0.25X) where X is transmission line reactance and x_c as 1.9Ω respectively. With these values there is only one resonant point at $\alpha = 139.75^\circ$, firing angle is set initially at 146° , which lies on the capacitive region of TCSC. After running load flow program X_{TCSC} is equal to -0.0319 pu and the final firing angle value is 149.029° with 7 iterations. Table (2) gives power flow results of 9-bus test system with and without TCSC, while fig.8 shows reactance-firing angle characteristics. From table (2) real power flow in line 7-8 at sending end increased from 76.38 MW to 80 MW.

Case IV:

TCSC is connected between bus 9 and bus 8, the control aim is to increase the real power flows in line 9-8 to 26 MW. The of values X_C and X_L are chosen as 13.33Ω pu and 2.67Ω with these values there is only one resonant point at $\alpha = 139.75^\circ$, firing angle is set initially at 146° , which lies on the capacitive region of TCSC . After running load flow program X_{TCSC} is equal to -0.0439 and the final firing angle value is 149.24° , with 6 iterations. Table (2) gives power flow results, and reactance-firing angle characteristics are illustrated in fig.8. From table (2) real power flow in line 9-8 at sending end increased from 24.18 MW to 26 MW.

Table (2) power flow results of 9-bus test system with and without TCSC

	Line	
	7-8	9-8
Final firing angle value (deg)	149.03	149.24
X_{TCSC} (pu)	-0.0319	-0.0439
Compensation (%)	-44.3	-43.6
Active power without TCSC(MW)	76.38	24.18
Active power with TCSC(MW)	80	26

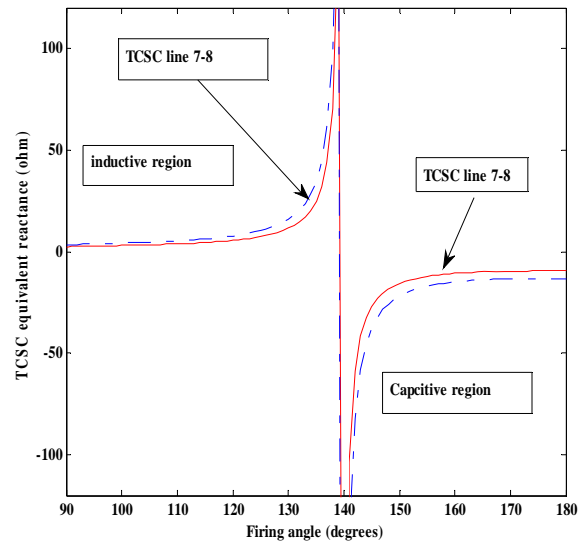


Fig.8 TCSC reactance-firing angle characteristics

VI. CONCLUSION

In this paper steady-state firing angle models of SVC and TCSC for power flow solution were developed and discussed in details. To demonstrate the effectiveness and robustness of the proposed models, a Newton-Raphson method incorporating firing angle model for SVC and TCSC was developed for desired power transferred and bus voltage profile improvement. Then the proposed models and algorithm were implemented on 9-bus test system for different case studies. The results obtained show the effectiveness and robustness of the proposed models; moreover the power solution using the Newton-Raphson algorithm developed incorporating firing angle model possesses excellent convergence characteristics.

ACKNOWLEDGMENT

The first author thanks Prof. S. J. Cheng for his valuable observations and suggestions. The research represented here has been supported by Huazhong University of Science and Technology (HUST).

REFERENCES

- [1] N.G. Hingorani, L. Gyugyi, "Understanding FACTS: Concepts and Technology of Flexible ac Transmission Systems", IEEE Press, New York, 1999.
- [2] Enrique Acha et al., "FACTS: Modeling and Simulation in Power Networks", Wiley, 2004.
- [3] A.Edris, "FACTS technology development: an update", IEEE Eng. Rev.20 (3), 2000, pp.4-9.
- [4] R.Mohan Marthur and Rajiv K.Varma "Thyristor Based-FACTS controllers for electrical transmission systems", Wiley, 2002.
- [5] Kirschner L.; Retzmann D.; Thumm G., "Benefits of FACTS for Power System Enhancement", Transmission and Distribution Conference and Exhibition: Asia and Pacific, 2005 IEEE/PES, pp.1 – 7.
- [6] Yan Ou; Chanan Singh, "Improvement of total transfer capability using TCSC and SVC", Power Engineering Society Summer Meeting, 2001. IEEE , Volume 2, 15-19 July 2001, pp. 944-948.

- [7] Perez M.A., Messina A.R., Fuerte-Esquivel C.R., "Application of FACTS devices to improve steady state voltage stability", Power Engineering Society Summer Meeting, 2000. IEEE, Volume 2, 16-20 July 2000, pp.1115 – 1120.
- [8] Xingbin Yu; Chanan Singh; Jakovljevic S.; Ristanovic D.; Garng Huang;" Total transfer capability considering FACTS and security constraints" Transmission and Distribution Conference and Exposition, 2003 IEEE PES-Volume 1, 7-12 Sept. 2003, pp.73 - 78 .
- [9] Pilotto L.A.S., Ping W.W., Carvalho A.R., Wey A., Long W.F., Alvarado F.L., Edris A., "Determination of needed FACTS controllers that increase asset utilization of power systems", Power Delivery, IEEE Transactions on, Jan. 1997, Volume: 12, Issue: 1, pp 364 – 371.
- [10] Narayana Prasad Padhy and M.A. Abdel Moamen," Power flow control and solutions with multiple and multi-type FACTS devices", Electric Power Systems Research, Vol.74, 2005, pp. 341-351.
- [11] Douglas J. Gotham, G. T. Heydt" Power flow control and power flow studies for systems with FACTS devies", IEEE Transactions on Power Systems, Vol. 13, No. 1, February 1998, pp.60 – 65.
- [12] P Yan and A.Sekar,"steady state analysis of power system having multiple FACTS devices using line-flow based equations",IEEE Pro. Transm. Distrib., vol,152,No.1 ,January 2005, pp. 31 – 39.
- [13] C.R. Fuerte-Esquivel, E. Acha,"Newton-Raphson algorithm for the reliable solution of large power networks with embedded FACTS devices",IEEE Pro.-Gener. Transm. Distrib., vol,143,No.5 ,Sep 1996, pp. 447-454.
- [14] Ying Xiao, Y.H. Song and Y.Z. Sun,"Power flow control approach to power systems with embedded FCATS devices",IEEE transaction on power systems, vol,17, No.4 ,Nov. 2002, pp. 943 – 950.
- [15] Paul M. Anderson, A. A. Fouad," Power System Control and Stability", Ieee Press Power Engineering Series, 2003.

BIOGRAPHIES



Mohammed Osman Hassan was born in Sinkat- Sudan in 1968; he received his Diploma and his Bachelor degree in Electrical Engineering, and his Master degree in Power System from Sudan University of Science and Technology –Sudan in 1992, 1997 and 2003 respectively. Currently, he is a Ph.D student in Huazhong University of Science and Technology (HUST) - China. His main

research interests are power system control, power system stability analysis, FACTS devices and application of AI in power systems.



S. J. Cheng (M'87–SM'88), Senior Member, IEEE, graduated from the Xi'an Jiao tong University, Xi'an, China, in 1967. He received the M.E. degree from the Huazhong University of Science and Technology (HUST), Wuhan, China, in 1981, and the Ph.D. degree in electrical engineering from the University of Calgary, Calgary, AB, Canada, in 1986. Currently, he is a Full Professor at HUST. His research interests are power system

control, power system stability analysis, and application of AI in power systems.



Zakaria Anwar Zakaria was born on Nov.1969 in Omdurman -Sudan. He graduated with M.Sc. degree from Vinnitsa Technical University, Faculty of Electrical Engineering in 1995 (Ukraine), then he received another M.Sc. in Renewable Energy Technology, Khartoum University – Sudan (2002). He is a lecturer in El-Imam El-Mahdy University, Faculty of Engineering and Technical Studies. Currently, he is a Ph.D Student in Wuhan

University, School of Electrical Engineering, His main research interests are power system analysis, power electronics technology, FACTS devices, and application of AI in power systems and renewable energy technology.